Propagation of a Tropical Cyclone in a Meridionally Varying Zonal Flow: An Energetics Analysis

BIN WANG AND XIAOFAN LI

Department of Meteorology, School of Ocean and Earth Science and Technology, University of Hawaii at Manoa, Honolulu, Hawaii

(Manuscript received 27 September 1993, in final form 10 October 1994)

ABSTRACT

Tropical cyclone propagation (the beta drift) is driven by a secondary circulation associated with axially asymmetric gyres (beta gyres) in the vicinity of the cyclone center. In the presence of the beta effect, the environmental flow may interact with the symmetric circulation and beta gyres of the cyclone, affecting the development of the gyres and thereby the cyclone propagation. An energetics analysis is carried out to elucidate the development mechanism of the beta gyres and to explain variations in propagation speed of a barotropic cyclone embedded in a meridionally varying zonal flow on a beta plane. Two types of zonal flows are considered: one with a constant meridional shear resembling those in the vicinity of a subtropical ridge or a monsoon trough, and the other with a constant relative vorticity gradient as in the vicinity of an easterly (westerly) jet.

Zonal flow with a constant meridional shear changes the generation rate of the gyre kinetic energy through an exchange of energy directly with the gyres. The momentum flux associated with gyres acting on the meridional shear of zonal flow accounts for this energy conversion process. Zonal flow with an anticyclonic (cyclonic) shear feeds (extracts) kinetic energy to (from) the gyres. The magnitude of this energy conversion is proportional to the strength of the meridional shear and the gyre intensity. As a result, the gyres are stronger and the beta drift is faster near a subtropical ridge (anticyclonic shear) than within a monsoon trough (cyclonic shear).

Zonal flow with a constant relative vorticity gradient affects gyre intensity via two processes that have opposing effects. A southward vorticity gradient, on the one hand, weakens the gyres by reducing the energy conversion rate from symmetric circulation to gyres; on the other hand, it enhances the gyres by indirectly feeding energy to the symmetric circulation, whose strengthening in turn accelerates the energy conversion from symmetric circulation to gyres. The effect of the second process tends to eventually become dominant.

1. Introduction

Tropical cyclone motion normally differs from an environmental steering (George and Gray 1976; Chan and Gray 1982; Carr and Elsberry 1990). The difference is attributed to a propagation component that arises from the interaction of the tropical cyclone circulation with embedded environment. Current understanding of the nature of the propagation is primarily gained from theoretical and numerical modeling studies.

Theoretically, the translation of an initially axially symmetric vortex embedded in a spatially varying environmental flow may be advantageously partitioned into two components: a steering caused by the advection of axially symmetric vorticity by the environmental flow, and a propagation induced by the advection of the symmetric vorticity by axially asymmetric flows near the vortex center. The asymmetric flows result from interactions between the vortex circulation and the planetary vorticity gradient (the beta effect) and the relative vorticity gradient of the environmental flow.

An example of pure steering was given by Adem and Lezama (1960), who showed that a barotropic symmetric vortex embedded in a uniform environmental flow on an f plane moves precisely with the uniform flow. An example of pure propagation was first studied by Rossby (1948), who showed that the beta effect can drive a rigid-body rotation cyclone northward in the absence of environmental flows. Recent numerical investigations have established that in a quiescent environment on a beta plane, the propagation of a barotropic symmetric vortex (the beta drift) is determined by the advection of symmetric vorticity by the asymmetric flow between a pair of counterrotating gyres (the beta gyres); the beta gyres are generated by the advection of planetary vorticity by the symmetric vortex circulation (Chan and Williams 1987; Willoughby 1988; Fiorino and Elsberry 1989; Peng and Williams 1990; Shapiro and Ooyama 1990; Smith et al. 1990; Li and Wang 1994; and others).

In the presence of both the beta effect and environmental flows, vortex translation is a combination of steering and propagation. In the simplest case, in which the environmental flow is uniform and time indepen-

Corresponding author address: Dr. Bin Wang, School of Ocean and Earth Science and Technology, University of Hawaii, 2525 Correa Rd., Honolulu, HI 96822.

dent, the movement of a barotropic vortex can be viewed simply as the sum of a steering by the environmental flow and a beta drift. When the environmental flow varies with latitude (as will be studied in this paper) or varies with time and space in general, it not only steers the vortex but also interacts with the vortex circulation, modifying the beta gyres and affecting propagation.

Sasaki (1955) and Kasahara (1957) found that an environmental relative vorticity gradient can force a cyclone to propagate in a direction 90° to the left of the relative vorticity gradient. DeMaria (1985) showed that an environmental absolute vorticity gradient may cause a cyclone to deviate from steering flow with one component in the direction of the gradient and another 90° to the left of the gradient. To isolate the effect of the environmental relative vorticity gradient on vortex motion, Ulrich and Smith (1991) designed an experiment on an f plane in which the environmental flow has a constant meridional relative vorticity gradient that equals β. They revealed that the poleward drift speed of a cyclone in such an environmental flow is much smaller than that of the same cyclone in a quiescent environment on a β plane, although the environmental absolute vorticity gradients are the same in the two cases. Williams and Chan (1994) further carried out two β-plane experiments in which the zonal flows have a constant relative vorticity gradient of $-\beta$ and β, so that the environmental absolute vorticity gradient is zero and 2β, respectively. In order to focus on the effects of relative vorticity gradient of the zonal flow on cyclone movement, they removed a steering component from the total displacement and obtained a propagation component that describes the deviation of the cyclone track from the steering current. They found that the propagation is faster in the case with zero vorticity gradient, but slower in the case with 2β vorticity gradient than the beta drift in the absence of environmental flow. The cause was not addressed.

A meridionally varying environmental flow may affect propagation even in the absence of the relative vorticity gradient. Ulrich and Smith (1991) and Smith (1991) examined the effect of a zonal flow with a constant vorticity (or meridional shear) on vortex motion on a beta plane. They found that the northward propagation in a zonal flow with an anticyclonic shear is significantly larger than that in a zonal flow with a cyclonic shear. Williams and Chan (1994) repeated this experiment. After subtracting the advection by environmental flow, they observed that the propagation in the cases with constant cyclonic and anticyclonic shear flows has the same orientation as the pure beta drift; however, the propagation in the cyclonic shear flow is slightly slower, whereas in the anticyclonic shear flow it is significantly faster than the pure beta drift. Again, what accounts for these differences is unclear.

The purpose of this paper is to elucidate the mechanisms by which meridionally varying zonal flows affect vortex propagation on a beta plane. A typical environmental pressure field in the troposphere consists of a subtropical ridge and a monsoon trough to its south. The corresponding zonal wind varies with latitude as illustrated in Fig. 1. Near a subtropical ridge and a monsoon trough, the zonal flow can be idealized as a linear function of latitude, whereas in the region of an easterly jet between the subtropical ridge and monsoon trough, the zonal flow may be approximately described by a sum of a parabolic function of latitude and a uniform easterly flow. It follows that two elementary meridionally varying zonal flows are interesting. One is a zonal flow with a constant meridional shear, and the other is a zonal flow with a constant relative vorticity gradient. Since the propagation is in accord with the evolution of the asymmetric gyres for both constant shear and constant vorticity gradient cases (Williams and Chan 1994), a central question is how these meridionally varying zonal flows affect the intensities of the asymmetric gyres and modify cyclone propagation speed. Sections 3 and 4 will address this question through energetics analyses. The kinetic energy equations of the gyres needed by the analysis will first be derived in the next section. The last section gives a summary.

2. The model and kinetic energy equations

a. The numerical model

To discuss barotropic motion of an initial symmetric vortex, we use a nonlinear shallow-water model. The governing equations in Cartesian coordinates are

$$\frac{\partial}{\partial t} U + U\cdot\nabla U + fk \times U = -\nabla\phi, \quad (2.1a)$$

$$\frac{\partial}{\partial t}\phi + \nabla\cdot(\phi U) = 0, \quad (2.1b)$$

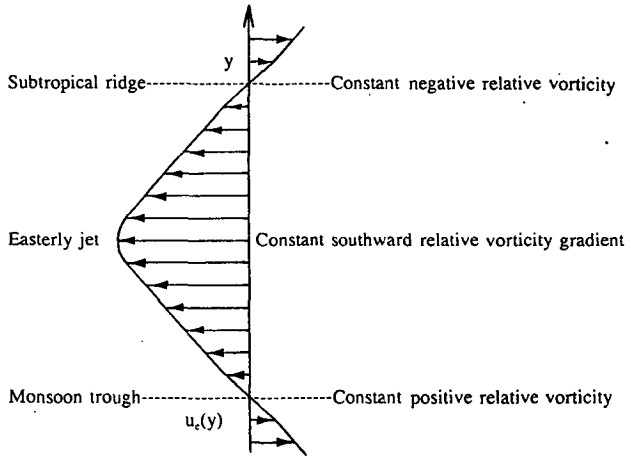

FIG. 1. Schematic variations of a zonal flow with latitude typical for a tropical cyclone environment.

where U and ϕ are, respectively, the horizontal wind and geopotential, and the Coriolis parameter f varies with latitude.

In order to assess the effect of a meridionally varying zonal flow on vortex motion, it is convenient to assume that the total wind consists of a time-independent environmental flow (U_e) and a time-varying vortex circulation (U_v):

$$U = U_v + U_e. \tag{2.2a}$$

Correspondingly, the geopotential consists of a vortex (ϕ_v) and an environmental component (ϕ_e):

$$\phi = \phi_v + \phi_e. \tag{2.2b}$$

Assume that the environmental flow satisfies Eqs. (2.1a) and (2.1b). Substituting (2.2) into (2.1) yields governing equations for the vortex circulation:

$$\frac{\partial}{\partial t} U_v + U\cdot\nabla U_v + fk \times U_v + \nabla\phi_v = -U_v\cdot\nabla U_e, \tag{2.3a}$$

$$\frac{\partial}{\partial t} \phi_v + \nabla\cdot(\phi_v U_v) = -\nabla\cdot(\phi_e U_v) - \nabla\cdot(\phi_v U_e). \tag{2.3b}$$

The terms on the right-hand sides of (2.3a) and (2.3b) involve interactions between the environmental flow and vortex circulation.

The numerical code is a modified version of the shallow-water model originally developed by Li and Zhu (1991). An integration domain of 6000 × 6000 km^2 is chosen with a square mesh of 40 km. Sponge layers described in Wang and Li (1992) are used along lateral boundaries. The meridionally varying environmental flow is in geostrophic balance with environmental geopotential. The initial vortex center for all cases is set at 20°N and is located where environmental flows are zero. Since the work of Adem (1956) it has been well known that the vortex propagation critically depends on vortex structure. To identify and focus on the effect of environmental flows, we used an initial vortex structure in which the azimuthal wind profile (Fig. 2) is defined by

$$v_\lambda(r) = \begin{cases} V_m \dfrac{r}{r_m}\left\{\exp\left[1 - \left(\dfrac{r}{r_m}\right)\right] - \dfrac{|r - r_m|}{R_0 - r_m}\exp\left[1 - \left(\dfrac{R_0}{r_m}\right)\right]\right\} & r \leqslant R_0, \\ 0 \quad r > R_0, \end{cases} \tag{2.4}$$

where $V_m = 30$ m s^{-1} is the maximum wind, $r_m = 100$ km the radius of maximum wind, and $R_0 = 750$ km the radius of the vortex circulation.

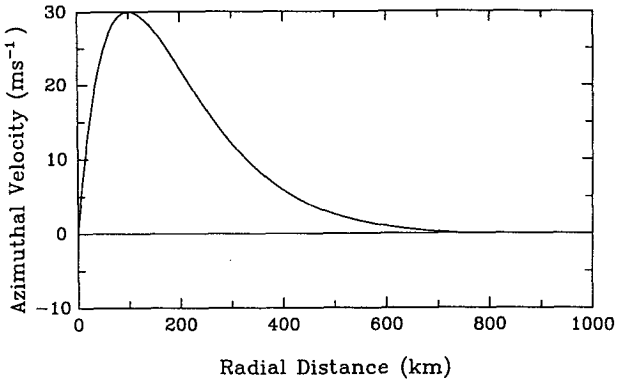

FIG. 2. Azimuthal wind profile of initial symmetric vortex.

In the model (2.3a,b), the zonal flow is specified. If the environmental flow is not fixed, it would vary with time, and the vortex movement would be different from that obtained in the present model. Our sensitivity tests revealed that the vortex tracks obtained from a model that allows temporal variation of environmental flows are just slightly different from those derived from the present model for the simple zonal flows studied in sections 3 and 4. This indicates that the temporal variations of the chosen environmental flows have no significant effect on vortex propagation. One should realize, however, that this conclusion holds only for those special cases studied in sections 3 and 4 in which the specified zonal flows are steady solutions of the governing equations. If the initial environmental flow is not a steady solution, the results obtained from the models with time-dependent and time-independent environmental flows could differ from each other significantly. Since we use model (2.3), in which the environmental flow is fixed, the effect of a specified environmental flow on vortex propagation can be assessed without ambiguity.

b. Kinetic energy equations

To elucidate the kinetic energy source of the development of the gyres, a set of kinetic energy equations for vortex circulation is derived. In the present study the divergent wind is negligible compared to the rotational wind. Thus, the rotational wind is used to approximately represent the total wind. The vortex circulation consists of a symmetric vortex (U_s) and an asymmetric circulation. The latter can further be partitioned into an azimuthal wavenumber 1 component, called a generalized beta gyre (U_g), and a residual (U_{res}) in terms of Fourier decomposition in the azimuthal direction. Thus, the vortex circulation

$$U_v = U_s + U_g + U_{\text{res}}. \tag{2.5}$$

The kinetic energy budgets are calculated over the whole model domain. Due to the circular nature of the

vortex circulation, the kinetic energy and the related conversion terms over the model domain (S) can be approximately obtained by integrations over a circular domain $A(t)$ with a radius R; that is,

$$\langle(\ \ )\rangle = \int_S\int (\ \ )dS = \int_{A(t)}\int (\ \ )dA$$
$$= \int_0^R rdr \int_0^{2\pi} (\ \ )d\lambda. \qquad (2.6)$$

Here the center of $A(t)$ is collocated with the center of moving cyclone, but the radius R of $A(t)$ is constant. The choice of the radius (R) of the integration domain is not unique. We choose R where the vortex circulation vanishes. Sensitivity tests indicated that for both constant shear and constant vorticity gradient cases the calculated energy budgets have no significant difference when R is between 1600 and 2000 km. Thus, R = 1600 km is chosen in the following computations. This lack of sensitivity to the choice of a large integration domain was also shown by Shapiro and Ooyama (1990) in their analysis of the angular momentum budget of an isolated vortex on a beta plane.

Multiplying Eq. (2.3a) by U_s, U_g, and U_{res}, respectively, integrating the resulting equations over the circular domain defined above, and using vector identity $A\cdot(B\times C) = B\cdot(C\times A) = C\cdot(A\times B)$ yield

$$\left\langle U_s\cdot\frac{\partial}{\partial t}U_v\right\rangle = -\langle(U\cdot\nabla U_s)\cdot U_s\rangle - \langle(U\cdot\nabla U_g)\cdot U_s\rangle - \langle(U\cdot\nabla U_{res})\cdot U_s\rangle$$
$$- \langle fk\cdot(U_{res}\times U_s)\rangle - \langle fk\cdot(U_g\times U_s)\rangle - \langle U_s\cdot\nabla\phi_v\rangle - \langle(U_v\cdot\nabla U_e)\cdot U_s\rangle, \qquad (2.7a)$$

$$\left\langle U_g\cdot\frac{\partial}{\partial t}U_v\right\rangle = -\langle(U\cdot\nabla U_s)\cdot U_g\rangle - \langle(U\cdot\nabla U_g)\cdot U_g\rangle - \langle(U\cdot\nabla U_{res})\cdot U_g\rangle$$
$$- \langle fk\cdot(U_{res}\times U_g)\rangle - \langle fk\cdot(U_s\times U_g)\rangle - \langle U_g\cdot\nabla\phi_v\rangle - \langle(U_v\cdot\nabla U_e)\cdot U_g\rangle, \qquad (2.7b)$$

$$\left\langle U_{res}\cdot\frac{\partial}{\partial t}U_v\right\rangle = -\langle(U\cdot\nabla U_s)\cdot U_{res}\rangle - \langle(U\cdot\nabla U_g)\cdot U_{res}\rangle - \langle(U\cdot\nabla U_{res})\cdot U_{res}\rangle$$
$$- \langle fk\cdot(U_g\times U_{res})\rangle - \langle fk\cdot(U_s\times U_{res})\rangle - \langle U_{res}\cdot\nabla\phi_v\rangle - \langle(U_v\cdot\nabla U_e)\cdot U_{res}\rangle. \qquad (2.7c)$$

To further simplify (2.7), we need the following vector identities:

$$\langle(A\cdot\nabla B)\cdot C\rangle = \langle A\cdot\nabla(B\cdot C)\rangle - \langle(A\cdot\nabla C)\cdot B\rangle, \qquad (2.8a)$$

$$\langle(A\cdot\nabla B)\cdot B\rangle = \frac{1}{2}\langle A\cdot\nabla(B\cdot B)\rangle, \qquad (2.8b)$$

and

$$\langle U\cdot\nabla G\rangle = \langle\nabla\cdot(UG)\rangle. \qquad (2.8c)$$

Equation (2.8c) is valid for any scalar G because the wind divergence $\nabla\cdot U$ is negligible. Note that the symmetric circulation, the gyres, and the residual are orthogonal with respect to each other in the sense that the integrations of the product of any two of them over the circular domain are zero. Using (2.8) in (2.7) yields a set of kinetic energy equations:

$$\frac{\partial K_s}{\partial t} = F_s - (K_s, K_g) - (K_s, K_{res}) + (K_e, K_g), \qquad (2.9a)$$

$$\frac{\partial K_g}{\partial t} = F_g + (K_s, K_g) + (K_{res}, K_g) + (K_e, K_g), \qquad (2.9b)$$

$$\frac{\partial K_{res}}{\partial t} = F_{res} + (K_s, K_{res}) - (K_{res}, K_g) + (K_e, K_{res}), \qquad (2.9c)$$

where

$$K_s = \frac{1}{2}\langle U_s\cdot U_s\rangle, \quad K_g = \frac{1}{2}\langle U_g\cdot U_g\rangle,$$
$$K_{res} = \frac{1}{2}\langle U_{res}\cdot U_{res}\rangle \qquad (2.10a)$$

are kinetic energy of the symmetric circulation, gyres, and residual circulation, respectively,

$$(K_s, K_g) = -\langle(U\cdot\nabla U_s)\cdot U_g\rangle + \langle fk\cdot(U_g\times U_s)\rangle, \qquad (2.10b)$$

$$(K_s, K_{res}) = -\langle(U\cdot\nabla U_s)\cdot U_{res}\rangle + \langle fk\cdot(U_{res}\times U_s)\rangle, \qquad (2.10c)$$

$$(K_{res}, K_g) = -\langle(U\cdot\nabla U_{res})\cdot U_g\rangle + \langle fk\cdot(U_g\times U_{res})\rangle, \qquad (2.10d)$$

$$(K_e, K_s) = -\langle(U_v\cdot\nabla U_e)\cdot U_s\rangle, \qquad (2.10e)$$

$$(K_e, K_g) = -\langle(U_v\cdot\nabla U_e)\cdot U_g\rangle, \qquad (2.10f)$$

$$(K_e, K_{res}) = -\langle(U_v\cdot\nabla U_e)\cdot U_{res}\rangle \qquad (2.10g)$$

are kinetic energy conversion terms, and

$$F_g = -\langle\nabla\cdot[UK_s]\rangle - \langle\nabla\cdot[U(U_g\cdot U_s)]\rangle - \langle\nabla\cdot[U(U_{\text{res}}\cdot U_s)]\rangle - \langle\nabla\cdot(U_s\phi_v)]\rangle, \quad (2.10h)$$

$$F_g = -\langle\nabla\cdot[UK_g]\rangle - \langle\nabla\cdot(U_g\phi_v)]\rangle, \quad (2.10i)$$

$$F_{\text{res}} = -\langle\nabla\cdot[UK_{\text{res}}]\rangle - \langle\nabla\cdot[U(U_g\cdot U_{\text{res}})]\rangle - \langle\nabla\cdot(U_{\text{res}}\phi_v)]\rangle \quad (2.10j)$$

are radial energy fluxes evaluated at the boundaries of the integration domain.

For convenience of calculation and analysis, we can introduce local cylindrical coordinates whose origin is at the cyclone center. The conversion terms in Cartesian coordinates (2.10b)–(2.10g) can be transformed into the following forms in the cylindrical coordinates (see appendix):

$$(K_s, K_g) = -\langle(V\cdot\nabla V_s)\cdot V_g\rangle + \langle f_1 k\cdot(V_g\times V_s)\rangle, \quad (2.11a)$$

$$(K_s, K_{\text{res}}) = -\langle(V\cdot\nabla V_g)\cdot V_{\text{res}}\rangle + \langle f_1 k\cdot(V_{\text{res}}\times V_s)\rangle, \quad (2.11b)$$

$$(K_{\text{res}}, K_g) = -\langle(V\cdot\nabla V_{\text{res}})\cdot V_g\rangle + \langle f_1 k\cdot(V_g\times V_{\text{res}})\rangle, \quad (2.11c)$$

$$(K_e, K_s) = -\langle(V_v\cdot\nabla V_e)\cdot V_s\rangle - \langle\Omega_v k\cdot(V_e\times V_s)\rangle, \quad (2.11d)$$

$$(K_e, K_g) = -\langle(V_v\cdot\nabla V_e)\cdot V_g\rangle - \langle\Omega_v k\cdot(V_e\times V_g)\rangle, \quad (2.11e)$$

$$(K_e, K_{\text{res}}) = -\langle(V_v\cdot\nabla V_e)\cdot V_{\text{res}}\rangle - \langle\Omega_v k\cdot(V_e\times V_{\text{res}})\rangle, \quad (2.11f)$$

where $f_1 = f + \Omega$, $\Omega = v_\lambda/r$ and $\Omega_v = v_{\lambda v}/r$; v_λ and $v_{\lambda v}$ are, respectively, the azimuthal components of the total flow (V) and the vortex flow (V_v) in the cylindrical coordinates.

Adding (2.9a)–(2.9c) yields a total kinetic energy equation for the vortex circulation:

$$\frac{\partial K_v}{\partial t} = F_v + (K_e, K_s) + (K_e, K_g) + (K_e, K_{\text{res}}). \quad (2.12)$$

Equation (2.12) indicates that the energy of total vortex circulation varies with time due to kinetic energy transfer between the environmental flow and the vortex circulation.

3. Development of the beta gyres in a zonal flow with a constant meridional shear

Three experiments were conducted. Case C_0 has a resting environment. Cases C_1 and C_2 have a zonal flow with a constant meridional shear (or constant relative vorticity):

$$u_e(y) = -\zeta_e(y - y_0). \quad (3.1)$$

This is an idealization of the zonal flow in the vicinity of a subtropical ridge ($\zeta_e < 0$, or anticyclonic shear) or a monsoon trough ($\zeta_e > 0$, or cyclonic shear) located at $y = y_0$. We assume that an initial vortex is centered at $y = y_0$ and ζ_e is -5.875×10^{-6} s^{-1} in case C_1 and 5.875×10^{-6} s^{-1} in case C_2.

As mentioned in section 1, the movement of a vortex embedded in an environmental flow consists of a steering and a propagating component. When the environmental flow is steady, the steering component can be readily computed. In a zonal flow with a constant meridional shear the environmental steering flow exactly equals the environmental flow at the vortex center. To examine the propagation caused by the asymmetric gyres, the steering component is first removed from the total vortex track. The resultant track is referred to as a propagation track. The propagation tracks of the vortices for both constant shear cases (Fig. 3) are similar to those of Williams and Chan (1994). Notice that case C_2 is also similar to the INMTR case of Evans et al. (1991), and the result is in good agreement with theirs. The total distance of propagation in the negative vorticity case (case C_1) is considerably greater than that in the resting environment case (case C_0), whereas in the positive vorticity case (case C_2) it is slightly less. Correspondingly, the propagation speeds in cases C_1, C_0, and C_2 at hour 48 are 3.49, 2.34, and 2.05 m s^{-1}, respectively. These experiments demonstrate that even without a relative vorticity gradient, a meridionally

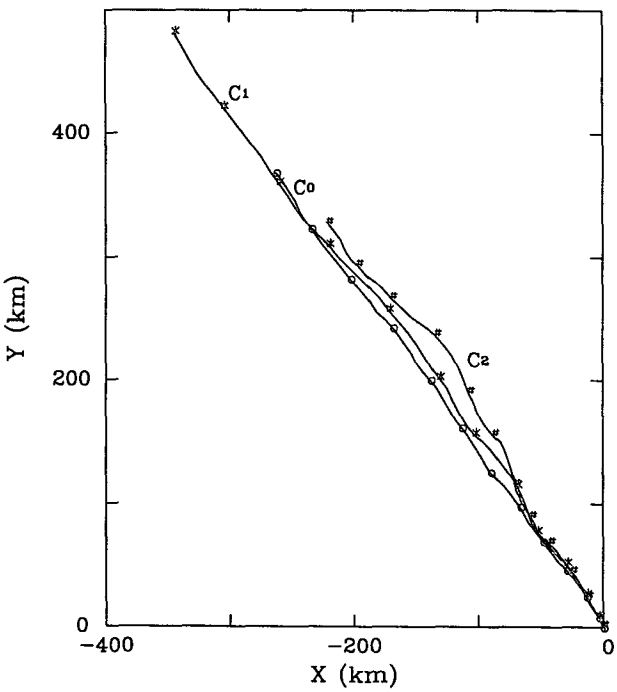

FIG. 3. The propagation tracks of the vortices at 6-h intervals for the constant anticyclonic shear case C_1 (*), the resting environment case C_0 (O), and the constant cyclonic shear case C_2 (#).

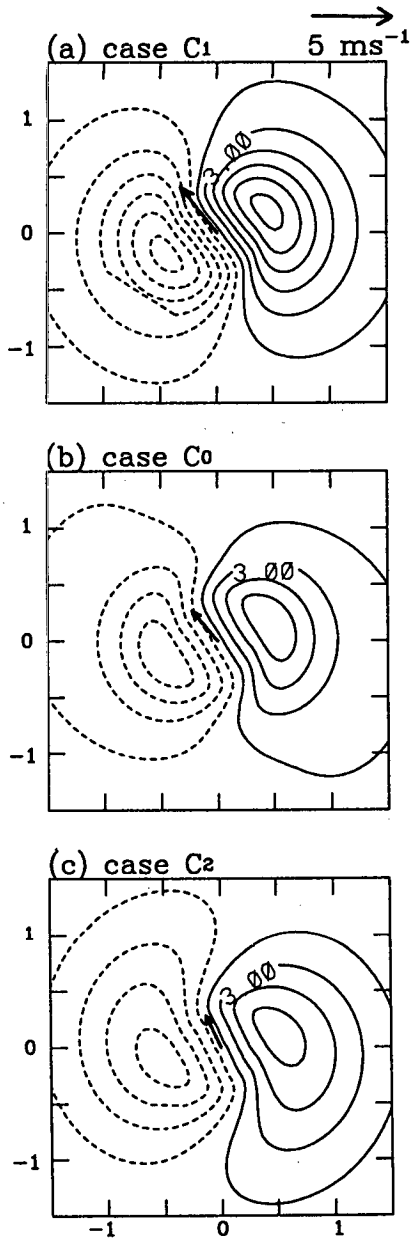

FIG. 4. The streamfunctions of the asymmetric gyres at hour 48 with a contour interval of 2×10^5 m^2 s^{-1} for (a) the constant anticyclonic shear case C_1, (b) the resting environment case C_0, and (c) the constant cyclonic shear case C_2. The arrow at the vortex center denotes the propagation velocity of the vortex. Abscissa and ordinate units are 1000 km.

varying zonal flow can affect the propagation if the beta effect exists.

The presence of the beta effect creates beta gyres. The presence of the constant shear zonal flow can change the intensity of the beta gyres. This can be seen from Fig. 4. In the anticyclonic shear case (case C_1) the intensity of the beta gyres is significantly stronger than that in the resting environment case (case C_0), whereas in the cyclonic shear case (case C_2) it is slightly weaker. The speed of vortex propagation is in good agreement with the averaged asymmetric flow (ventilation flow) in the vicinity of the vortex center (Fig. 4). The ventilation flow was obtained by averaging asymmetric flows over a circular area with 200-km radius where the relative vorticity of the symmetric vortex is positive for the chosen vortex profile. At hour 48, the differences in the speeds between the propagation and ventilation flow are less than 0.2 m s^{-1}. The strength of the ventilation flow is determined by the intensity of the asymmetric gyres. What, then, causes the differences in the intensity of the gyres?

The intensity of the asymmetric gyres can be measured in terms of the amount of kinetic energy because of the dominance of rotational wind component and the circular nature of the gyres. For this reason, we examine the kinetic energy budget at hour 48 (Fig. 5). The changes in propagation speeds in cases C_1 and C_2 are consistent with the changes in the gyre kinetic en-

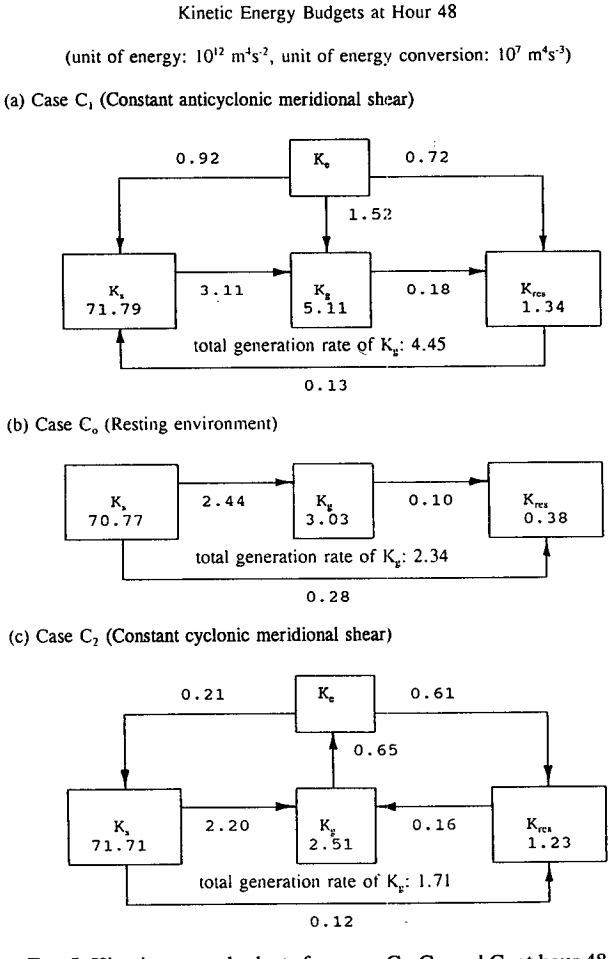

FIG. 5. Kinetic energy budgets for cases C_1, C_0, and C_2 at hour 48. The values in boxes denote the energy in units of 10^{12} m^4 s^{-2}, and the other values represent the energy conversions in units of 10^7 m^4 s^{-3}. The arrows indicate direction of energy transfer.

ergy (GKE) K_g (or the intensity of the gyres). Figure 5 indicates that in the presence of a zonal flow with a constant shear, the energy transfer between the gyres and the residual asymmetric flow is negligible; two energy conversion processes account for the difference in the K_g between cases C_1 and C_2. The first is the kinetic energy conversion between the zonal environmental flow and the gyres (K_e, K_g). The kinetic energy is converted from the zonal flow to the gyres in case C_1 (Fig. 5a), whereas it is converted from the gyres to the zonal flow in case C_2 (Fig. 5c). The second is the kinetic energy conversion from the symmetric circulation to the beta gyres (K_s, K_g). The rate of kinetic energy conversion from the symmetric flow to the gyres is larger in case C_1, whereas it is smaller in case C_2 than in case C_0. As a result, the total rates of generation of the GKE in the anticyclonic shear case, the resting environment case, and the cyclonic shear case are, respectively, 4.45, 2.34, and 1.71 (in units of 10^7 m^4 s^{-3}). The difference in the generation rate of the GKE between cases C_1 and C_0 (2.11×10^7 m^4 s^{-3}) is larger than that between cases C_2 and C_0 (0.63×10^7 m^4 s^{-3}). Consequently, the differences in the gyre strengths and propagation speeds between cases C_1 and C_0 are also larger than those between cases C_2 and C_0.

It is important to understand how the presence of a zonal flow with a constant meridional shear can alter the energy conversion (K_e, K_g) and (K_s, K_g). We first focus on the term (K_s, K_g). In cylindrical coordinates, the constant shear zonal flow (3.1) can be expressed as

$$v_{re} = 0.5r\zeta_e \sin2\lambda, \tag{3.2a}$$

$$v_{\lambda e} = 0.5r\zeta_e(1 + \cos2\lambda). \tag{3.2b}$$

It thus has a symmetric and an azimuthal wavenumber 2 component and has no effect on the energy conversion (K_s, K_g), because $-\langle(V_e\cdot\nabla V_s)\cdot V_g - (v_{\lambda e}/r)k\cdot(V_g \times V_g)\rangle = 0$ in (2.11a). Therefore, the conversion (K_s, K_g) in the constant shear zonal flow has the same form as in a quiescent environment. Li and Wang (1994) have shown that in a quiescent environment on a beta plane the rate of the conversion (K_s, K_g) is primarily proportional to the strengths of the symmetric circulation and the beta gyres. Since the strengths of the symmetric circulations between cases C_1 and C_2 are about the same, the difference in the rates of the conversion (K_s, K_g) must result from the difference in the strengths of the beta gyres, which is caused, in the first place, by the corresponding difference in the kinetic energy conversion (K_e, K_g).

The conversion between K_e and K_g, therefore, is a key process determining the difference in the GKE between cases C_1 and C_2. It deserves further analysis. Substituting (3.1) into (2.10f) and neglecting the effect of the residual flow, we have

$$(K_e, K_g) = -\langle(U_v\cdot\nabla U_e)\cdot U_g\rangle = \zeta_e\langle u_g v_s\rangle + \zeta_e\langle u_\epsilon v_g\rangle. \tag{3.3}$$

In the local cylindrical coordinates,

$$u_g = -v_{rg}\sin\lambda - v_{\lambda g}\cos\lambda, \tag{3.4a}$$

$$v_g = v_{rg}\cos\lambda - v_{\lambda g}\sin\lambda, \tag{3.4b}$$

$$v_s = -v_{\lambda s}\sin\lambda, \tag{3.4c}$$

where λ is the azimuthal phase angle; v_{rg} and $v_{\lambda g}$ are, respectively, the radial and azimuthal component of the gyres. Therefore,

$$\langle u_g v_s\rangle = 0.5\langle v_{rg}v_{\lambda s} - (v_{rg}\cos2\lambda - v_{\lambda g}\sin2\lambda)v_{\lambda s}\rangle = 0, \tag{3.5}$$

and (3.3) reduces to

$$(K_e, K_g) = \zeta_e\langle u_g v_g\rangle. \tag{3.6}$$

Equation (3.6) indicates that the gyre momentum flux (or Reynolds stress), $\langle u_g v_g\rangle$, acting on the meridional shear of the zonal flow represents a kinetic energy conversion mechanism for constant shear zonal flow cases. For the beta gyres in the constant shear cases C_1 and C_2 (Fig. 4), the gyre momentum flux $\langle u_g v_g\rangle < 0$. For a zonal flow with an anticyclonic shear ($\zeta_e < 0$), the Reynolds stress associated with the gyres extracts energy from zonal flow, causing development of the gyres. In this case, the gyres are "learning" against the zonal flow. For a zonal flow with a cyclonic shear ($\zeta_e > 0$), the gyre momentum flux converts kinetic energy from the gyres to zonal flow so that the gyres weaken.

Further, using (3.4a) and (3.4b), Eq. (3.6) can be rewritten as

$$(K_e, K_g) = -0.5\zeta_e\langle(v_{rg}^2 - v_{\lambda g}^2)\sin2\lambda + 2v_{rg}v_{\lambda g}\cos2\lambda\rangle. \tag{3.7}$$

Equation (3.7) can also be derived from (2.11e) with the use of (3.2a,b).

For simplicity, the streamfunction of the gyres is approximately expressed by

$$\psi_g = R_g(r)\cos(\alpha - \lambda), \tag{3.8}$$

where R_g is the amplitude of the gyres and α the azimuthal angle of the anticyclonic gyre center measured counterclockwise from due north. Here α is independent of the radial distance so that the effect of the varying radial phase tilt of the gyres is not considered. Substituting (3.8) into (3.7) yields

$$(K_e, K_g) = 0.5\zeta_e \sin2\alpha K_g. \tag{3.9}$$

In the constant shear cases C_1 and C_2, the anticyclonic gyre center is located in the northeast quadrant of the cyclone center so that $\sin2\alpha < 0$. Therefore, the following inferences can be made from (3.9).

1) The sign of conversion from K_e to K_g is determined by the sign of the meridional shear. An anticyclonic shear allows a kinetic energy conversion from

the environmental flow to the beta gyres (case C_1 in Fig. 5), whereas a cyclonic shear favors kinetic energy transferring from the gyres to the environmental flow (case C_2 in Fig. 5).

2) The rate of conversion between K_e and K_g is proportional to the magnitude of the environmental meridional shear. In the zonal flows with an anticyclonic shear of 2.94×10^{-6}, 5.875×10^{-6}, and 11.75×10^{-6} s^{-1} the propagation speeds at hour 48 are 2.73, 3.49, and 4.36 m s^{-1}, respectively, indicating that a stronger anticyclonic shear favors stronger gyre development and faster propagation. On the other hand, with increasing magnitude of a cyclonic shear, the generation rate of the GKE decreases, and the propagation speed decreases accordingly. For instance, in the zonal flows with a cyclonic shear of 2.94×10^{-6}, 5.875×10^{-6}, and 11.75×10^{-6} s^{-1} the propagation speeds at hour 48 are 2.20, 2.05, and 1.67 m s^{-1}, respectively.

3) The rate of conversion from K_e to K_g is approximately proportional to K_g. Therefore, if this conversion mechanism operates alone, it would cause an exponential growth or decay of K_g. Since K_g is affected by symmetric vortex structure, the kinetic energy conversion (K_e, K_g) also depends on the structure of symmetric vortex circulation. For instance, in the same zonal flow with a negative relative vorticity of -5.875×10^{-6} s^{-1} the propagation speed at hour 48 increases from 3.32 to 3.66 m s^{-1} when the vortex size R_0 increases from 600 to 900 km; it increases from 2.09 to 4.73 m s^{-1} when the maximum wind speed of the cyclone V_m increases from 15 to 45 m s^{-1}. The sensitivity of propagation speed to the maximum wind of the symmetric cyclone shown here is due to the fact that for the azimuthal wind profile of symmetric cyclone (2.4) the change in the maximum wind induces significant change in the outer flow of symmetric cyclone.

4. Development of the gyres in a zonal flow with a constant relative vorticity gradient

We now consider a zonal flow that has a constant meridional gradient of relative vorticity β_e; that is,

$$u_e = -0.5\beta_e(y - y_0)^2. \quad (4.1)$$

Addition of a uniform easterly (westerly) environmental flow to a negative (positive) β_e represents an ideal easterly (westerly) jet centered at $y = y_0$. The values of β_e in cases D_1 and D_2 are deliberately chosen as $-\beta$ and β at y_0 (20°N), respectively, so that the environmental absolute vorticity gradient is zero in case D_1 and 2β in case D_2.

In a zonal flow with a constant relative vorticity gradient, the environmental steering depends not only on the environmental flow at the vortex center but also on the size of the positive vorticity area of the cyclone. Consider that a cyclone is centered at $y = y_c$. The environmental steering (u_{es}) may be defined by the mean flow averaged over a circular area centered at the vortex center and with a radius of r_0. The calculations result is

$$u_{es} = -0.5\beta_e(y_c - y_0)^2 - 0.125\beta_e r_0^2. \quad (4.2)$$

Thus, the environmental steering is not precisely equal to the environmental flow at the vortex center; it also contains a term that is a quadratic function of r_0. If one takes the positive symmetric vorticity area as the area over which the environmental flow is averaged, r_0 should be 200 km for the chosen vortex structure shown in Fig. 2. The difference in environmental steering between $r_0 = 0$ and $r_0 = 200$ km is about ± 0.11 m s^{-1}. In general, the environmental steering in the parabolic jet flow depends on the initial symmetric vortex structure and the definition of the steering current itself. In the following we determine environmental steering by taking $r_0 = 200$ km.

Figure 6 shows the propagation tracks for cases D_1 and D_2 during a 108-h integration. These tracks are different from those displayed by Williams and Chan (1994) because they simply took the zonal flow at the vortex center as the environmental steering. The propagation direction in case D_2 is close to that in case C_0,

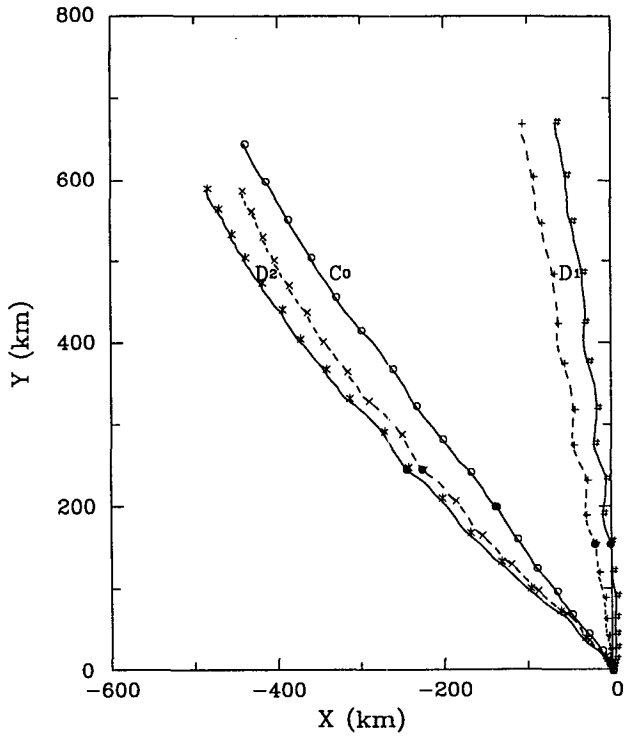

FIG. 6. The propagation tracks of the vortices at 6-h intervals for cases D_1, C_0, and D_2. Solid lines with # and *, respectively, represent the tracks relative to environmental steering defined at the vortex center for cases D_1 and D_2. Dashed lines with + and ×, respectively, denote the tracks relative to environmental steering defined by averaging over the circular area with 200-km radius for cases D_1 and D_2. Solid line with ○ is the track for case C_0. Here ● denotes the positions of vortex centers at hour 48.

but the propagation in case D_1 is directed more northward. The variations of propagation speeds in both cases are similar to those found by Williams and Chan (1994).

An interesting difference between cases D_1 and D_2 is that the vortex in case D_1 moves slower than that in case D_2 in the first 48 h, but faster in the last 48 h. The propagation speeds for cases D_1, C_0, and D_2 are, respectively, 0.72, 1.23, and 2.29 m s^{-1} at hour 24, while they are 2.82, 2.63, and 1.46 m s^{-1} at hour 96. The variation in the propagation speed results from the intensity variation of the gyres (Fig. 7). At hour 24, the gyres in case D_1 are weaker than those in case D_2. At hour 96, however, the gyres in case D_1 become much stronger than those in case D_2. The intensity of the gyres corresponds very well to the amount of GKE (Figs. 8a,b). To interpret the difference in the evolution of the gyre intensity, we can diagnose the generation of the GKE.

Figures 8a and 8b show that the generation rate of the GKE is primarily determined by the balance between (K_s, K_g) and (K_e, K_g). In both cases, (K_s, K_g) is a source while (K_e, K_g) is a sink for the GKE. The difference in total generation rate of the GKE between cases D_1 and D_2 is mainly attributed to the marked difference in (K_s, K_g) between the two cases: From hour 24 to hour 96, there is a dramatic increase of (K_s, K_g) in case D_1 but a significant decrease of (K_s, K_g) in case D_2. What causes this difference? To answer this question, we analyze the conversion (K_s, K_g).

The conversion from K_s to K_g given by (2.10b) can be rewritten as

$$(K_s, K_g) = CT_1 + CT_2 + CT_2^*, \qquad (4.3)$$

where

$$CT_1 = -\langle (U_g \cdot \nabla U_s) \cdot U_g \rangle, \qquad (4.4a)$$

$$CT_2 = \langle \beta y k \cdot (U_s \times U_g) \rangle, \qquad (4.4b)$$

$$CT_2^* = -\langle (U_e \cdot \nabla U_s) \cdot U_g \rangle. \qquad (4.4c)$$

Here term CT_1 represents the conversion associated with the advection of symmetric circulation by the gyres, and term CT_2 results from the beta effect. Terms CT_1 and CT_2 are, respectively, identical to the nonlinear conversion and the beta conversion in the absence of the environmental flow (Li and Wang 1994). Term CT_2^* denotes an additional nonlinear conversion associated with advection of symmetric circulation by the environmental flow.

At hour 24, (K_s, K_g) in case D_2 is nearly twice large as that in case D_1 (Fig. 8a). Table 1 shows the breakdown of the contribution from the three terms on the right-hand side of (4.3). The difference in (K_s, K_g) between cases D_1 and D_2 is primarily due to the opposite sign of CT_2^*. Thus, a zonal flow with a northward (southward) relative vorticity gradient enhances

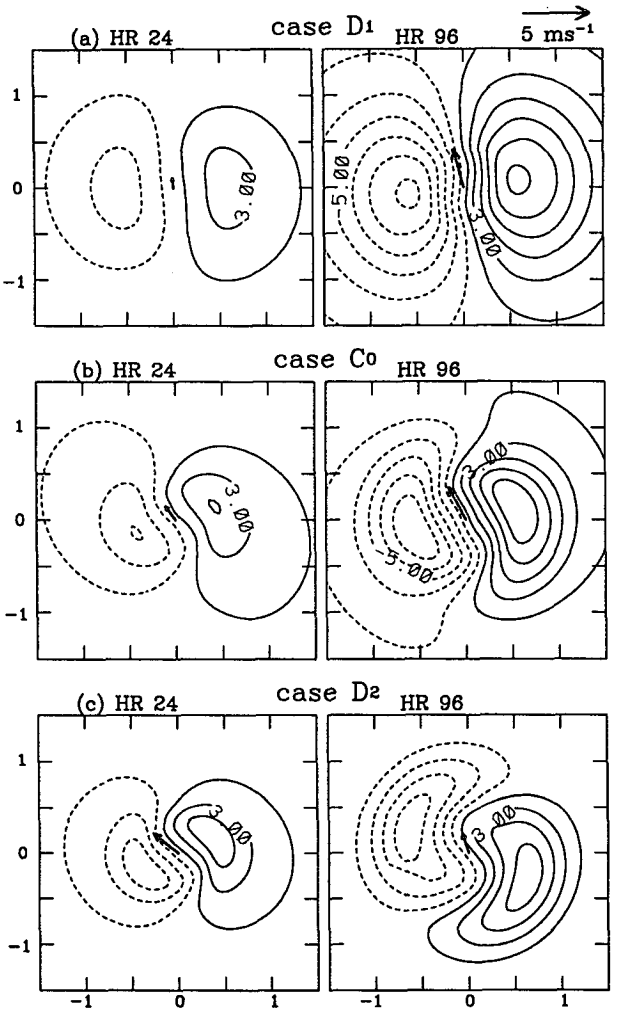

FIG. 7. The streamfunctions of the asymmetric gyres at hour 24 and hour 96 with a contour interval of 2×10^5 m^2 s^{-1} for (a) case D_1, (b) case C_0, and (c) case D_2. The arrow at the vortex center denotes the propagation velocity of the vortex. Abscissa and ordinate units are 1000 km.

(reduces) the GKE by directly accelerating (decelerating) the rate of the conversion (K_s, K_g).

At hour 96, on the contrary, (K_s, K_g) in case D_1 is almost twice large as that in case D_2 (Fig. 8b). Although the southward relative vorticity gradient in case D_1 strongly prohibits the conversion of kinetic energy from the symmetric circulation to the gyres (CT_2^*), the enormous increase in the beta conversion (CT_2) in case D_1 dominates, so that (K_s, K_g) in case D_1 is much larger than that in case D_2 (Table 1). In the previous study of Li and Wang (1994), we have shown that the (K_s, K_g) increases as the symmetric circulation intensifies. In case D_1 the symmetric circulation continuously extracts kinetic energy from the environmental flows, whereas in case D_2 the symmetric circulation feeds ki-

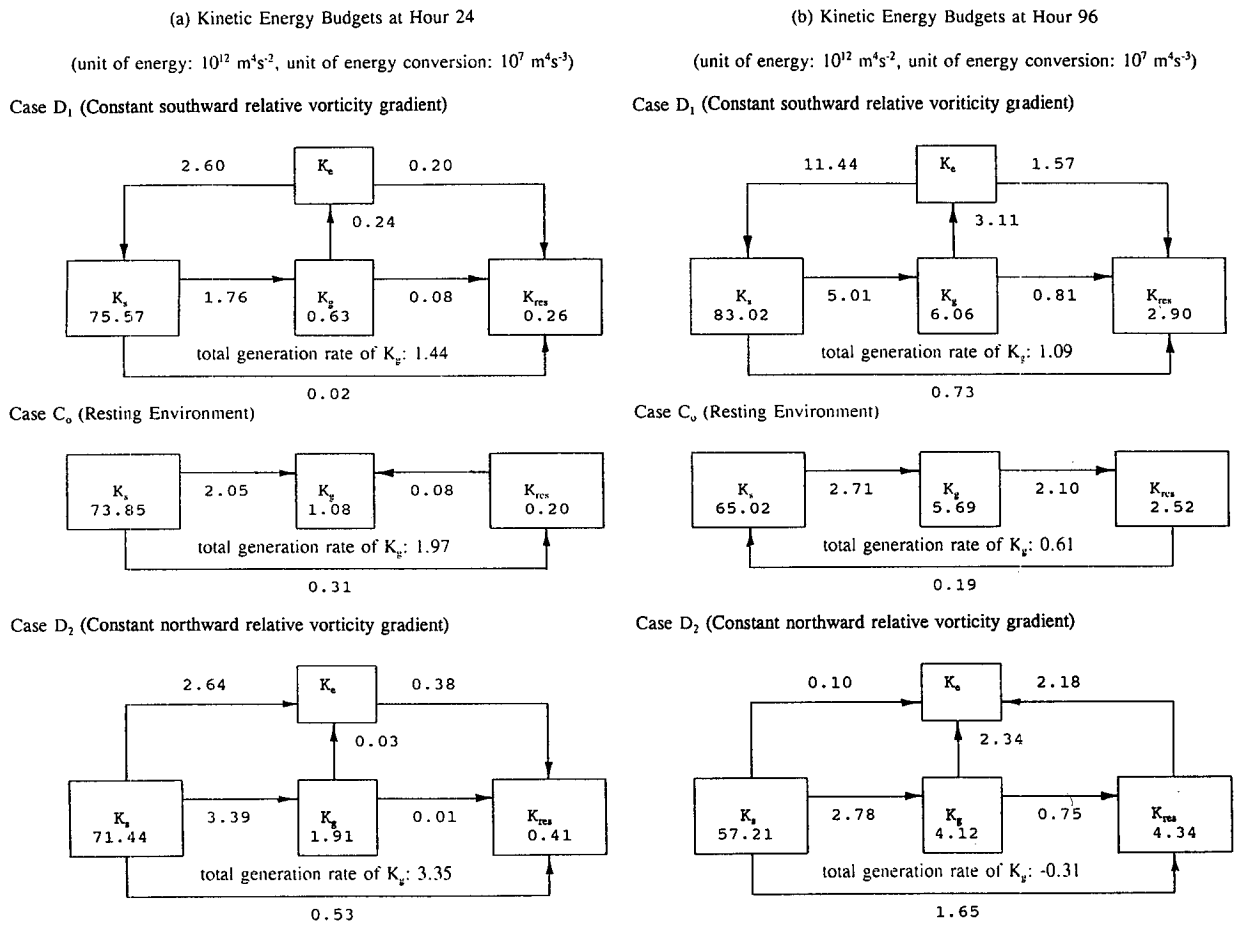

FIG. 8. Kinetic energy budgets for cases D_1, C_0, and D_2 at (a) hour 24 and (b) hour 96. The values in boxes denote the energy in units of 10^{12} m^4 s^{-2}, and the other values represent the energy conversions in units of 10^7 m^4 s^{-3}. The arrows indicate direction of energy transfer.

netic energy back to the environmental flow. Thus, the symmetric vortex in case D_1 becomes much stronger than that in case D_2 by hour 96. Consequently, the rate of energy conversion from the symmetric circulation to the gyres in case D_1 becomes nearly twice large as that in case D_2. A zonal flow with a southward vorticity gradient enhances the GKE by indirectly feeding the energy to the symmetric circulation, whose strengthening in turn accelerates the rate of the energy conversion from the symmetric circulation and the beta gyres.

TABLE 1. The breakdown of (K_s, K_g) in cases D_1, C_0, and D_2 at (a) hour 24 and (b) hour 96 (unit: 10^7 m^4 s^{-1}). See (4.4) for the definitions of CT_1, CT_2, and CT_2^*.

(a) Case	CT_1	CT_2	CT_2^*
D_1	−0.04	2.53	−0.73
C_0	−0.50	2.55	0.00
D_2	−0.50	2.76	1.13
(b) Case	CT_1	CT_2	CT_2^*
D_1	−1.99	13.24	−6.24
C_0	−0.45	3.16	0.00
D_2	−0.15	2.01	0.92

The conversion (K_e, K_s) is analyzed to elucidate how a zonal flow with a constant vorticity gradient changes the strength of the symmetric circulation. Considering a quadratic zonal flow and neglecting the effect of the residual flow, (2.10e) can be expressed by

$$(K_e, K_s) = -\langle (U_v \cdot \nabla U_e) \cdot U_s \rangle = -\left\langle \frac{\partial u_e}{\partial y} u_s v_s \right\rangle - \left\langle \frac{\partial u_e}{\partial y} u_s v_g \right\rangle. \quad (4.5)$$

Using (3.4c) and

$$u_s = -v_{\lambda s} \cos\lambda, \quad (4.6a)$$

$$\frac{\partial u_e}{\partial y} = -\beta_e r \cos\lambda, \quad (4.6b)$$

we can show that

$$-\left\langle \frac{\partial u_e}{\partial y} u_s v_s \right\rangle = 0.5\beta_e \langle r v_{\lambda s}^2 \cos\lambda \sin 2\lambda \rangle = 0. \quad (4.7)$$

Thus, (4.5) becomes

$$(K_e, K_s) = -\left\langle \frac{\partial u_e}{\partial y} u_s v_g \right\rangle. \quad (4.8)$$

Equation (4.8) indicates that in a zonal flow with a constant relative vorticity gradient the energy conversion between the environmental flow and the symmetric vortex is determined by the interactions among the relative vorticity of the zonal flow, the zonal wind component of the symmetric circulation, and the meridional wind component of the gyres.

Substituting (3.4b), (4.6a), and (4.6b) into (4.8) yields

$$(K_e, K_s) = -\beta_e \langle r v_{\lambda s} \cos^2\lambda (v_{rg} \cos\lambda - v_{\lambda g} \sin\lambda) \rangle. \quad (4.9)$$

Note that (4.9) can also be derived from (2.11d) by inserting the cylindrical coordinate form of the zonal flow (4.1):

$$v_{re} = 0.125\beta_e r^2 (\sin\lambda + \sin 3\lambda), \quad (4.10a)$$

$$v_{\lambda e} = 0.125\beta_e r^2 (3\cos\lambda + \cos 3\lambda). \quad (4.10b)$$

Assume that the streamfunction of the gyres has the same approximation as in (3.8). Using (3.8) in (4.9) yields

$$(K_e, K_s) = -0.25\pi\beta_e \left[\sin\alpha \int_0^R R_g r^3 \frac{\partial}{\partial r} \left(\frac{v_{\lambda s}}{r} \right) dr \right]. \quad (4.11)$$

For both cases D_1 and D_2, the asymmetric anticyclonic gyre is located to the east of the cyclone center so that $\sin\alpha < 0$. The azimuthal angular wind ($v_{\lambda s}/r$) decreases with increasing radial distance for the given vortex profile so that the integration in (4.11) is also negative. It follows that the value in the square bracket is positive. Thus, in case D_1 (with a negative β_e) the kinetic energy is transferred from K_e to K_s, whereas in case D_2 (with a positive β_e) the energy is converted from K_s to K_e.

Finally, we notice that the intensification (in case D_1) and decay (in case D_2) of the symmetric vortex do not depend on whether the environmental flow satisfies the necessary condition for barotropic instability. This suggests that the nonlinear evolution of the symmetric vortex cannot be interpreted by the linear barotropic instability theory. Chan and Williams (1987) also found that linear theory was not able to explain the nonlinear evolution of the symmetric and asymmetric components of the vortex.

5. Summary

The mechanism by which meridionally varying steady zonal flows affect cyclonic vortex propagation in the presence of planetary vorticity gradient is studied using kinetic energy analysis in a shallow-water model.

In a uniform zonal flow the vortex propagation is the same as the beta drift of the vortex in a quiescent environment; the beta gyres grow by extracting kinetic energy from the symmetric circulation, and their intensity determines the vortex propagation speed. In a meridionally varying zonal flow, there are two major kinetic energy transfer processes: the conversion between the symmetric circulation and the gyres, and the conversion between the environmental flow and the gyres.

In a zonal environmental flow with an anticyclonic meridional shear, the beta gyres intensify more rapidly than without environmental flow by extracting extra energy from the zonal flow. As a result, the vortex propagates significantly faster than in the absence of the zonal flow. The opposite is true for the cyclonic shear case. Therefore, the presence of constant meridional shear can effectively modify the beta gyres and change cyclonic propagation speed. For the development of the beta gyres, the exchange of kinetic energy between the zonal flow and the beta gyres is a key process. The mechanism responsible for this energy exchange is that the gyres transport momentum flux to reduce the meridional shear of the zonal flow.

In a zonal environmental flow with a constant relative vorticity gradient, the primary energy source for the development of the beta gyres is the conversion from the symmetric circulation to the beta gyres. The environmental relative vorticity gradient affects the strength of the beta gyres by directly changing the energy conversion rate from the symmetric vortex to the gyres (K_s, K_g) and by indirectly changing the energy conversion rate between the environmental flow and the symmetric vortex. The presence of a northward (southward) relative vorticity gradient in the zonal flow, on the one hand, enhances (reduces) the (K_s, K_g). Thus, in the beginning the gyres are stronger and the vortex propagates faster in the case of a northward relative vorticity gradient (case D_2) than in the case of a southward vorticity gradient (case D_1). On the other hand, the presence of a northward (southward) relative vorticity gradient weakens (strengthens) the symmetric vortex by transferring (extracting) energy to (from) the zonal flow. This process leads to an enhanced symmetric circulation in case D_1 and a weakened one in case D_2 in the later stages (after 48 h). Because the major portion of the (K_s, K_g) is in proportion to the strength of the symmetric vortex, the conversion rate (K_s, K_g) in case D_1 becomes much larger than that in case D_2 in the late stage. As a result the gyres are stronger and the vortex propagates faster in case D_1 than in case D_2 at hour 96.

The results here imply that in the vicinity of a steady monsoon trough (subtropical ridge) where a constant cyclonic (anticyclonic) relative vorticity exists, the beta drift will be slower (faster). Similar results in the vicinity of the steady monsoon trough were found by Evans et al. (1991) in their INMTR case. In the vicinity of an easterly jet between the subtropical ridge and monsoon trough, where a southward relative vorticity gradient exists, the beta drift may be accelerated due to the strengthening of the symmetric vortex. The above conclusions are confined to a situation in which the longitudinal and temporal variations of the environmental flows are not significant.

When the zonal and meridional length scales of the environmental flow are comparable, zonal variations of the meridional component of the environmental flow may have significant effects on the beta gyres and vortex propagation. The propagation of a vortex embedded in a zonally varying meridional flow and an environmental flow that has both zonal and meridional components requires further investigation.

Acknowledgments. We thank Dr. T. A. Schroeder for his comments, Y. Wang for his original code of the shallow-water model, and anonymous reviewers for providing helpful comments on an earlier version of this manuscript. This research is supported by the Marine Meteorology Program of the Office of Naval Research under Grant N00014-90-J-1383.

APPENDIX

Transformation of the Energy Conversion Terms from Cartesian to Cylindrical Coordinates

Express wind in the cylindrical coordinates as

$$V = i_r v_r + i_\lambda v_\lambda, \tag{A1a}$$

and in Cartesian coordinates as

$$U = iu + jv, \tag{A1b}$$

where v_r and v_λ denote the radial and azimuthal wind components, respectively; i_r and i_λ are, respectively, the unit vectors in the radial and azimuthal directions; u and v represent the zonal and meridional wind components, respectively; and i and j are, respectively, the unit vectors in the zonal and meridional directions.

To show that the conversion terms (2.11a)–(2.11f) are identical to those in Cartesian coordinates (2.10b)–(2.10g), it is sufficient to show

$$-(V_1\cdot\nabla V_2)\cdot V_3 - \Omega_1 k\cdot(V_2\times V_3) = -(U_1\cdot\nabla U_2)\cdot U_3, \tag{A2}$$

where $\Omega_1 = v_{\lambda 1}/r$, and subscripts 1, 2, and 3 represent the symmetric, gyre, and residual components in any order.

Using (A1), the terms on the lhs and rhs of (A2) can be respectively expressed as

$$\begin{aligned}-(V_1\cdot\nabla V_2)\cdot V_3 - \Omega_1 k\cdot(V_2\times V_3) &= -\left(v_{r1}\frac{\partial v_{r2}}{\partial r} + v_{\lambda 1}\frac{\partial v_{r2}}{r\partial\lambda}\right)v_{r3} \\ &\quad -\left(v_{r1}\frac{\partial v_{\lambda 2}}{\partial r} + v_{\lambda 1}\frac{\partial v_{\lambda 2}}{r\partial\lambda}\right)v_{\lambda 3} \\ &\quad -\frac{v_{\lambda 1}}{r}(v_{r2}v_{\lambda 3} - v_{\lambda 2}v_{r3}),\end{aligned} \tag{A3a}$$

and

$$\begin{aligned}-(U_1\cdot\nabla U_2)\cdot U_3 &= -\left(u_1\frac{\partial u_2}{\partial x} + v_1\frac{\partial u_2}{\partial y}\right)u_3 \\ &\quad -\left(u_1\frac{\partial v_2}{\partial x} + v_1\frac{\partial v_2}{\partial y}\right)v_3.\end{aligned} \tag{A3b}$$

Because

$$v_r = -u\sin\lambda + v\cos\lambda, \tag{A4a}$$

$$v_\lambda = -u\cos\lambda - v\sin\lambda, \tag{A4b}$$

where λ is an azimuthal angle measured from due north counterclockwise, and

$$\frac{\partial}{\partial r} = -\sin\lambda\frac{\partial}{\partial x} + \cos\lambda\frac{\partial}{\partial y}, \tag{A5a}$$

$$\frac{\partial}{r\partial\lambda} = -\cos\lambda\frac{\partial}{\partial x} - \sin\lambda\frac{\partial}{\partial y}, \tag{A5b}$$

using (A4) and (A5) and the identity $\sin^2\lambda + \cos^2\lambda = 1$ leads to

$$\begin{aligned}-\left(v_{r1}\frac{\partial v_{r2}}{\partial r} + v_{\lambda 1}\frac{\partial v_{r2}}{r\partial\lambda}\right) + \frac{v_{\lambda 1}}{r}v_{\lambda 2} &= \left(u_1\frac{\partial u_2}{\partial x} + v_1\frac{\partial u_2}{\partial y}\right)\sin\lambda \\ &\quad -\left(u_1\frac{\partial v_2}{\partial x} + v_1\frac{\partial v_2}{\partial y}\right)\cos\lambda\end{aligned} \tag{A6a}$$

$$\begin{aligned}-\left(v_{r1}\frac{\partial v_{\lambda 2}}{\partial r} + v_{\lambda 1}\frac{\partial v_{\lambda 2}}{r\partial\lambda}\right) - \frac{v_{\lambda 1}}{r}v_{r2} &= \left(u_1\frac{\partial u_2}{\partial x} + v_1\frac{\partial u_2}{\partial y}\right)\cos\lambda \\ &\quad +\left(u_1\frac{\partial v_2}{\partial x} + v_1\frac{\partial v_2}{\partial y}\right)\sin\lambda.\end{aligned} \tag{A6b}$$

Finally, substituting (A4) and (A6) into (A3) yields (A2).

REFERENCES

Adem, J., 1956: A series solution for the barotropic vorticity equation and its application in the study of atmospheric vortices. *Tellus,* **8,** 364–372.

——, and P. Lezama, 1960: On the motion of a cyclone embedded in a uniform flow. *Tellus,* **8,** 364–372.

Carr, L. E., III, and R. L. Elsberry, 1990: Observational evidence for predictions of tropical cyclone propagation relative to environmental steering. *J. Atmos. Sci.,* **47,** 542–546.

Chan, J. C.-L., and W. M. Gray, 1982: Tropical cyclone movement and surrounding flow relationship. *Mon. Wea. Rev.,* **110,** 1354–1374.

——, and R. T. Williams, 1987: Analytical and numerical studies of the beta effect in tropical cyclone motion. Part I: Zero mean flow. *J. Atmos. Sci.,* **44,** 1257–1265.

DeMaria, M., 1985: Tropical cyclone motion in a nondivergent barotropic model. *Mon. Wea. Rev.,* **113,** 1199–1209.

Evans, J. L., G. J. Holland, and R. L. Elsberry, 1991: Interactions between a barotropic vortex and an idealized subtropical ridge. Part I: Vortex motion. *J. Atmos. Sci.,* **48,** 301–314.

Fiorino, M., and R. L. Elsberry, 1989: Some aspects of vortex structure related to tropical cyclone motion. *J. Atmos. Sci.,* **46,** 975–990.

George, J. E., and W. M. Gray, 1976: Tropical cyclone motion and surrounding parameter relationship. *J. Appl. Meteor.,* **15,** 1252–1135.

Kasahara, A., 1957: The numerical prediction of hurricane movement with the barotropic model. *J. Meteor.,* **14,** 386–402.

Li, T., and Y. Zhu, 1991: Analysis and modelling of tropical cyclone motion (I): The axiasymmetric structure and the sudden change of tracks. *Science in China,* Ser. B, **34,** 223–233.

Li, X., and B. Wang, 1994: Barotropic dynamics of the beta gyres and beta drift. *J. Atmos. Sci.,* **51,** 746–756.

Peng, M. S., and R. T. Williams, 1990: Dynamics of vortex asymmetries and their influence on vortex motion on a β plane. *J. Atmos. Sci.,* **47,** 1987–2003.

Rossby, C. G., 1948: On displacement and intensity changes of atmospheric vortices. *J. Mar. Res.,* **7,** 175–187.

Sasaki, Y., 1955: Barotropic forecasting for the displacement of a typhoon. *J. Meteor. Soc. Japan,* **32,** 1–8.

Shapiro, L. J., and K. V. Ooyama, 1990: Barotropic vortex evolution on a beta plane. *J. Atmos. Sci.,* **47,** 170–187.

Smith, R. K., 1991: An analytic theory of tropical-cyclone motion in a barotropic shear flow. *Quart. J. Roy. Meteor. Soc.,* **117,** 685–714.

——, W. Ulrich, and G. Dietachmayer, 1990: A numerical study of tropical cyclone motion using a barotropic model. Part I: The role of vortex asymmetries. *Quart. J. Roy. Meteor. Soc.,* **116,** 337–362.

Ulrich, W., and R. K. Smith, 1991: A numerical study of tropical cyclone motion using a barotropic model. II: Motion in spatially varying large-scale flows. *Quart. J. Roy. Meteor. Soc.,* **117,** 107–124.

Wang, B., and X. Li, 1992: The beta drift of three-dimensional vortices: A numerical study. *Mon. Wea. Rev.,* **120,** 579–593.

Williams, R. T., and J. C.-L. Chan, 1994: Numerical studies of the beta effect in tropical cyclone motion. Part II: Zonal mean flow effects. *J. Atmos. Sci.,* **51,** 1065–1076.

Willoughby, H. E., 1988: Linear motion of a shallow-water, barotropic vortex. *J. Atmos. Sci.,* **45,** 1906–1928.